Andreev-level tunneling in a ballistic double superconductor–normal-metal–superconductor junction

Victor C. Y. Chang and C. S. Chu
Department of Electrophysics, National Chiao Tung University, Hsinchu 30050, Taiwan, Republic of China
(Received 19 August 1996)

The supercurrent in a mesoscopic, ballistic, and symmetrically stacked, double superconductor–normal-metal–superconductor (SNS) junction is studied. Our focus is to establish the features in the supercurrent that are associated with the Andreev-level tunneling between the two SNS junctions. Both the junction geometry dependence and the gap function dependence are studied and are analyzed in terms of the quasiparticle scattering processes. The quasiparticle scattering is worked out analytically by solving the Bogoliubov–de Gennes equation within the Andreev approximation. The current is calculated, following Beenakker and van Houten [Phys. Rev. Lett. **66**, 3056 (1991)], and the result is found to differ from that of the transmission approach. Such discrepancy between the two approaches, however, is found to disappear for a single SNS junction. In our result, the currents in the two normal regions are checked to be the same. [S0163-1829(97)04309-9]

I. INTRODUCTION

The transport properties of mesoscopic systems with mixed normal (N) and superconducting (S) constituents have attracted much attention in recent years.[1] This is prompted partly by the potential physical phenomena in such systems and partly by the potential device applications using these systems. A number of physical phenomena have recently been predicted[2–5] and observed.[6,7] These include, in the dirty regime, the mesoscopic fluctuations of the critical current in a superconductor–normal-metal–superconductor (SNS) Josephson junction,[2,3] and, in the ballistic regime, the quantization of the critical current in a superconducting quantum point contact (SQPC).[4,5] The mesoscopic fluctuation in the critical current has physical origin closely associated with that of the universal conductance fluctuations in mesoscopic normal systems, which, essentially, is the manifestation of the phase coherence in the normal region. The quantization of the critical current, on the other hand, has physical origin closely associated with that of the quantized conductance in a normal quantum point contact, which is the quantization of the transverse energy in the SQPC. That the physical properties of a SQPC can be different from its *classical* counterpart, the *classical* superconducting point contact (SPC), of which the transverse dimension $W \gg \lambda_F$, is demonstrated by the quantization of the critical current not in a SPC, but in a SQPC. The distinct physical properties of mesoscopic superconducting nanostructures warrant further exploration effort worthwhile.

A simple mesoscopic superconducting nanostructure in the SNS Josephson-junction configuration has been considered in recent studies.[2–14] The SNS junction is a pair-potential well in which the quasiparticles are reflected, according to Andreev,[15] at the NS interfaces. An electronlike (holelike) excitation can be reflected at the NS interface and becomes a holelike (electronlike) excitation, while simultaneously transmitting (extracting) a Cooper pair to (from) the superconducting electrode. Repeated Andreev reflections between the two NS interfaces thus contribute to the supercurrent across the junction. Furthermore, for those quasiparticles with energies lower than the gap potential of the electrodes, they are confined within the well and form Andreev levels. We note that these Andreev levels contribute to the supercurrent, and are, by nature, different from the bound states in a quantum well.

Therefore, it is interesting to find ways to probe these Andreev levels. A proposal is made recently to induce transition between these levels by introducing a gate-induced time-dependent potential in the normal region.[16] We propose instead, in this paper, to probe the tunneling between Andreev levels from quantum transport measurement. The system we study is a double SNS (SNSNS) junction and the tunneling occurs between the levels in the two SNS junctions. Our focus is to establish the features in the supercurrent that are associated with the Andreev-level tunneling.

The transport characteristics of SNSNS junctions have also been considered recently.[17,18] Motivated by the possible macroscopic quantum analog between the resonant tunneling of Schrödinger electrons and the transmission of Cooper pairs, Zapata and Sols[17] consider two δ-profile barriers in a quasi-one-dimensional superconductor and argue that the δ-profile barriers, under certain conditions, behave like normal regions. The critical current is calculated within the Ginzburg-Landau (GL) regime, and the results show that, near the critical temperature T_c, the temperature dependence of the critical current differs markedly from that of a SNS junction. Moreover, from their results that the critical current becomes independent of the distance d between the junctions when $d \gg \xi(T)$, Zapata and Sols conclude that the analogy with the resonant tunneling is, in their wording,[17] at best qualitative. Here $\xi(T)$ is the coherence length of the superconductor at temperature T.

The GL approach, though interesting, cannot establish the connection between the supercurrent characteristics and the microscopic Andreev levels in the structure, and, in addition, is not appropriate for much lower temperatures. Taking a

 © 1997 The American Physical Society

microscopic approach, Hurd and Wendin study the supercurrent in the same structure using the Bogoliubov–de Gennes (BdG) equation.[18] The discrete spectrum of the excitations are calculated numerically by a transfer-matrix method. The supercurrent due to the scattering states is obtained from a Landauer-type formula in which the current is expressed in terms of the quasiparticle transmission coefficients. This transmission approach to the quantum transport has found great success in mesoscopic normal structures[19] and has been generalized to mesoscopic superconducting structures.[4,8,18,20–25] In the paper,[18] the connection between the current characteristics and the microscopic Andreev levels is not established. Furthermore, despite the intuitively appealing feature, the transmission approach to mesoscopic superconducting structures has not been formally verified, except for simple structures.[22] The important issue that remains is whether the quantum transport approach, which works well for Schrödinger particles in mesoscopic normal structures, can, in the present generalized form, work well also for quasiparticles in mesoscopic superconducting structures? This issue of analogy, or generalization, is, in spirit, similar to that brought forth by Zapata and Sols.[17] Since the SNSNS junction is the simplest nontrivial structure that might help shed light on this issue, we calculate, in this paper, the supercurrent in such structure using a microscopically derived current expression[4] and compare with the results using the transmission approach.

From our results, the current-phase relation (CPR) of a SNSNS junction, at zero temperature, has features of abrupt current change which is associated with the occurrence of Andreev levels at the chemical potential μ. The phase is the phase difference between the order parameters of the two superconductors at the ends of the structure. As the tunneling effects between the Andreev levels increase, either by decreasing the length or lowering the gap potential of the middle superconductor, we find that the phase separation between the two Andreev levels at μ increases. Consequently, the phase separation between the two abrupt-current-change features in the CPR increases, and the connection of the CPR with the Andreev-level tunneling is established. Encouraged by recent CPR measurement in superconducting weak links,[26,27] we expect the CPR characterization of mesoscopic superconducting structures to be possible in the near future. We also obtain the analytic expression for the supercurrent due to the scattering states, using both our approach and the transmission approach. The two expressions are different. Besides, from our numerical examples, the differences in the CPR and in the critical current are quite significant. This discrepancy between the two approaches, however, is found to disappear in a single SNS junction.

In Sec. II we present the formulation for the quasiparticle scattering and the supercurrent in a SNSNS junction. In Sec. III we present the analytic expressions for the quantization condition of the Andreev levels, and for the current due to the scattering states. Numerical examples for the supercurrent-phase relation, for the critical current and for the finite-temperature effects are presented. Finally, Sec. IV presents a conclusion.

II. THEORY

In this section, we outline the method for the calculation of the quasiparticle scattering states and the Andreev levels.

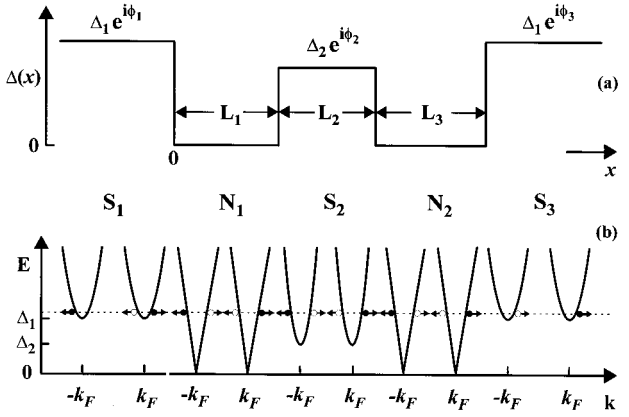

FIG. 1. (a) Schematic representation of a $S_1N_1S_2N_2S_3$ junction with stepwise pair potentials and (b) the dispersion relations for the excitations in respective regions. The case of an electronlike excitation (closed circle) incident from the left-hand side is shown. The open circles are the holelike excitations.

Both the current expressions used in our calculation and used in the transmission approach are presented. Explicit results for the SNSNS junctions are presented in the next section.

The $S_1N_1S_2N_2S_3$ junction, as shown in Fig. 1, is a one-dimensional channel, with the pair potential given by

$$\Delta(x)=\begin{cases}\Delta_1 e^{i\phi_1}, & x<0\\ 0, & 0<x<L_1\\ \Delta_2 e^{i\phi_2}, & L_1<x<L_1+L_2\\ 0, & L_1+L_2<x<L_1+L_2+L_3\\ \Delta_1 e^{i\phi_3}, & x>L_1+L_2+L_3.\end{cases} \tag{1}$$

The energy gap, Δ_1, of the superconducting electrodes at the two ends of the structure is taken to be the same but the phases of their respective pair potentials are different. The quasiparticles of the system are described by the BdG equation

$$\begin{bmatrix} H(x) & \Delta(x) \\ \Delta^*(x) & -H^*(x)\end{bmatrix}\begin{bmatrix} u(x)\\ v(x)\end{bmatrix}=E\begin{bmatrix} u(x)\\ v(x)\end{bmatrix}, \tag{2}$$

where $H(x)=p_x^2/2m-\mu$ is the single-electron Hamiltonian, and μ is the chemical potential, from which the quasiparticle energy E is defined, is assumed to be the same throughout the structure. The energy spectrum of the quasiparticles in different regions of the structure is shown in Fig. 1. We consider only $E>0$ because the quasiparticles are the excitations of the system.

In the normal regions N_j ($j=1,2$), the normalized eigenfunctions of Eq. (2) are

$$\Psi^{\pm}_{N_j,e}=\begin{bmatrix}1\\0\end{bmatrix}\exp(\pm i\tilde{k}_e x),$$

$$\Psi^{\pm}_{N_j,h}=\begin{bmatrix}0\\1\end{bmatrix}\exp(\pm i\tilde{k}_h x), \tag{3}$$

where $\tilde{k}_e=k_F\sqrt{1+E/\mu}$, $\tilde{k}_h=k_F\sqrt{1-E/\mu}$, and $k_F=\sqrt{2m\mu}/\hbar$. The subscript $e(h)$ indicates the electronlike

(holelike) quasiparticle. The superscript $\pm$ gives the group velocity direction of the electronlike quasiparticle but gives the direction opposite to the group velocity of the holelike quasiparticle. Similarly, in the superconductor regions S_j ($j=1,2,3$), the normalized eigenfunctions of Eq. (2) are

$$\Psi^{\pm}_{S_j,e}=\begin{bmatrix} u_j \exp(i\phi_j) \\ v_j \end{bmatrix} \exp(\pm i k_{e,j} x),$$

$$\Psi^{\pm}_{S_j,h}=\begin{bmatrix} v_j \exp(i\phi_j) \\ u_j \end{bmatrix} \exp(\pm i k_{h,j} x), \tag{4}$$

where

$$u_j^2=\frac{1}{2}\left(1+\frac{\sqrt{E^2-\Delta_j^2}}{E}\right), \quad v_j^2=\frac{1}{2}\left(1-\frac{\sqrt{E^2-\Delta_j^2}}{E}\right), \tag{5}$$

and

$$k_{e,j}=k_F\sqrt{1+\frac{\sqrt{E^2-\Delta_j^2}}{\mu}}, \quad k_{h,j}=k_F\sqrt{1-\frac{\sqrt{E^2-\Delta_j^2}}{\mu}}. \tag{6}$$

The above expressions can be analytically continued to include the case $E<\Delta_j$ by taking the branch $\sqrt{-|x|}=i\sqrt{|x|}$ for the square root. These eigenfunctions are used to construct the wave function of the entire structure. In the following, we take that $\Delta_3=\Delta_1$ and $\Delta_2 \leqslant \Delta_1$. The more general energy-gap configurations can be handled with the same method.

In the scattering regime, when $E>\Delta_1$, the quasiparticles are not confined. Thus the wave functions are the scattering states associated with quasiparticles incident from either side of the structure. The wave function, for example, for an electronlike quasiparticle incident from the left-hand side of the $S_1N_1S_2N_2S_3$ junction has the form

$$\Psi(x)=\begin{cases} \Psi^{+}_{S_1,e}+r_e\Psi^{-}_{S_1,e}+r_h\Psi^{+}_{S_1,h} & \text{in } S_1, \\ A_1\Psi^{-}_{N_1,e}+A_2\Psi^{-}_{N_1,h}+A_3\Psi^{+}_{N_1,h}+A_4\Psi^{+}_{N_1,e} & \text{in } N_1, \\ B_1\Psi^{-}_{S_2,e}+B_2\Psi^{-}_{S_2,h}+B_3\Psi^{+}_{S_2,h}+B_4\Psi^{+}_{S_2,e} & \text{in } S_2, \\ A_5\Psi^{-}_{N_2,e}+A_6\Psi^{-}_{N_2,h}+A_7\Psi^{+}_{N_2,h}+A_8\Psi^{+}_{N_2,e} & \text{in } N_2, \\ t_e\Psi^{+}_{S_3,e}+t_h\Psi^{-}_{S_3,h} & \text{in } S_3. \end{cases} \tag{7}$$

The normal process, in which the outgoing quasiparticle is still electronlike, is given by the coefficients r_e, t_e. The Andreev process, in which the outgoing quasiparticle is changed to holelike, is given by the coefficients r_h, t_h. All the coefficients are determined after matching the wave function at the NS boundaries. The matching is simplified by imposing the Andreev approximation in which all the wave vectors $\tilde{k}_e, \tilde{k}_h, k_{e,j}, k_{h,j}$ are approximated by k_F, except when they appear in the exponent. As a result, all the coefficients associated with eigenfunctions having superscript $-$ are dropped. The t_e and the r_h coefficients are found to satisfy $|t_e|^2+|r_h|^2=1$, and their respective expressions are given in Appendix A. The Andreev approximation is appropriate for $\mu \gg \Delta_1$. Other scattering states can be obtained similarly.

In the other regime, when $E \leqslant \Delta_1$, the quasiparticles are confined in the structure and the energies are quantized. Furthermore, when $E<\Delta_2$, the quasiparticles are confined within, but can tunnel between, the two normal regions. There are two kinds of bound states, according to the processes that set up the bound states. The first, called the p process,[28] is constructed from eigenstates having superscript $+$, which is associated with right-going electronlike quasiparticles in the normal regions. The second, called the n process,[28] is constructed from eigenstates having superscript $-$, and is associated with right-going holelike quasiparticles in the normal regions. The p-process wave function is given by[12]

$$\Psi(x)=\begin{cases} a\Psi^{+}_{S_1,h}/\sqrt{|u_1|^2+|v_1|^2} & \text{in } S_1, \\ C_1\Psi^{+}_{N_1,e}+D_1\Psi^{+}_{N_1,h} & \text{in } N_1, \\ (c\Psi^{+}_{S_2,e}+d\Psi^{+}_{S_2,h})/\sqrt{|u_2|^2+|v_2|^2} & \text{in } S_2, \\ C_2\Psi^{+}_{N_2,e}+D_2\Psi^{+}_{N_2,h} & \text{in } N_2, \\ b\Psi^{+}_{S_3,e}/\sqrt{|u_1|^2+|v_1|^2} & \text{in } S_3. \end{cases} \tag{8}$$

The n-process wave function can be obtained from Eq. (8) by changing the superscript $+$ to $-$ and the subscripts (e,h) to (h,e). The quantization condition is obtained after matching the wave function at all NS interfaces. Finally, the normalization of the wave function is used to determine all the coefficients.

With both the scattering states and the bound states determined, the supercurrent can be obtained using the current density expression

$$j(x)=\frac{e}{m}\sum_l \{f(E_l)u_l^*(x)\hat{p}_x u_l(x) + [1-f(E_l)]v_l(x)\hat{p}_x v_l^*(x)\}+\text{c.c.}, \tag{9}$$

where l refers to the quasiparticle states, continuous or discrete in energy spectrum, with $E_l>0$, and with the wave functions given by $[u_l(x),v_l(x)]^T$. Here $e=-|e|$, and $\hat{p}_x=-i\hbar d/dx-(e/c)A_x(x)$. The vector potential $A_x(x)=0$

in our case. The function $f(\epsilon)=[1+\exp(\epsilon/k_BT)]^{-1}$ is the Fermi function. In one dimension, the current density becomes the current. It is important to note that this current expression is microscopically derived, and has been applied to superconductors in previous works.[29,4] A detail derivation is presented in Appendix B. The current expression treats the scattering states and the bound states on the same footing. In our calculation, we evaluate the current in the normal regions. This approach to the current is rigorous, though, in practice, is not as convenient as the transmission approach. A comparison between the results from the two approaches should give a credible check on the latter approach.

For completeness, we give, in the following, the current expression that is used for the transmission approach,

$$I=I_1+I_2, \tag{10}$$

where

$$I_1=-\frac{2e}{\hbar}\sum_l \tanh(E_l/2k_BT)\frac{dE_l}{d\phi}, \tag{11}$$

is associated with the discrete levels,[4,18,31,32] and

$$I_2=-\frac{2e}{h}\int_{\Delta_1}^{\sqrt{\mu^2+\Delta_1^2}} dE\frac{E}{\sqrt{E^2-\Delta_1^2}}\tanh(E/2k_BT) \times[T^e_{L\to R}(E,\phi)-T^h_{L\to R}(E,\phi)], \tag{12}$$

is associated with the scattering states.[18] Here ϕ is the phase difference between the pair potentials of S_3 and S_1. The $T^{e(h)}_{L\to R}$ is the transmission coefficient for the right-going electronlike (holelike) quasiparticles.

III. RESULTS

In this section, we present the Andreev levels, the bound-state supercurrent, the scattering-state supercurrent, the current-phase relation, and the critical current of a symmetric SNSNS junction, of which the length of the two normal regions are the same, with $L_1=L_3=L$. The phases ϕ_1, and ϕ_3 of the two end superconductors are chosen to be $-\phi/2$, and $\phi/2$, respectively, while for the middle superconductor, we choose $\phi_2=0$. Thus ϕ is the phase difference across the junction. The supercurrent, given by Eq. (9), is found in this section to be the same in both of the normal regions.

A. Andreev levels

The quantization conditions for the Andreev levels are obtained according to the method outlined after Eq. (8). The conditions can be reduced to more compact expressions if we keep $\tilde{k}_e$ and $\tilde{k}_h$ up to the first order in E/μ, and $k_{e,j}$ and $k_{h,j}$ up to the first order in $\sqrt{E^2-\Delta_j^2}/\mu$. For the case $E\leqslant\Delta_2$, the conditions are

$$\left\{\cos\left[\frac{E}{\mu}k_FL-\cos^{-1}\left(\frac{E}{\Delta_1}\right)-\cos^{-1}\left(\frac{E}{\Delta_2}\right)\mp\frac{\phi}{2}\right]-1\right\} \times\exp\left(\frac{\sqrt{\Delta_2^2-E^2}k_FL_2}{2\mu}\right)-\left\{\cos\left[\frac{E}{\mu}k_FL-\cos^{-1}\left(\frac{E}{\Delta_1}\right) +\cos^{-1}\left(\frac{E}{\Delta_2}\right)\mp\frac{\phi}{2}\right]-1\right\}\exp\left(-\frac{\sqrt{\Delta_2^2-E^2}k_FL_2}{2\mu}\right)=0, \tag{13}$$

where the upper (lower) sign denotes the p process (n process). The phase dependence $E(\phi)$ of the Andreev levels has a period of 4π, because the phase appears only in the cosine functions, and as $\phi/2$. The exponential factors in Eq. (13) involve L_2 and represent the effects of tunneling on the Andreev levels. In the limit of infinite L_2, Eq. (13) becomes $Ek_FL/\mu-\arccos(E/\Delta_1)-\arccos(E/\Delta_2)\mp\phi/2=2\pi n$, which is the quantization conditions for an asymmetric SNS junction,[12] but with phase difference $\phi/2$. In another limit, when $E=0$, the quantization conditions become

$$\frac{\phi}{2}+2\pi n=\pi\pm\cos^{-1}\left[\tanh\left(\frac{\Delta_2k_FL_2}{2\mu}\right)\right], \tag{14}$$

from which the values of ϕ are determined. Surprisingly, Eq. (13) does not depend on both the energy gap Δ_1 of the superconducting electrodes and the length L of the normal regions. This means that the $E(\phi)$ features near $E=0$ remain the same for junctions with either long, or short, normal regions. It also implies that the phases ϕ, at which the Andreev level $E=0$, depend only on the middle superconductor. There are two such ϕ values in a 4π phase interval, when L_2 is finite. The phase separation $\Delta\phi_0$ between these two phases decreases as L_2 increases until the two phases coincide at 2π, when L_2 is infinite. The direct connection between $\Delta\phi_0$ and the Andreev-level tunneling is demonstrated.

For the case when $\Delta_2<E<\Delta_1$, the quantization conditions become

$$\left\{\cos\left[\frac{E}{\mu}k_FL-\cos^{-1}\left(\frac{E}{\Delta_1}\right)\mp\frac{\phi}{2}\right]-\frac{\Delta_2}{E}\right\}\sin\left(\frac{\sqrt{E^2-\Delta_2^2}k_FL_2}{2\mu}\right) +\sin\left[\frac{E}{\mu}k_FL-\cos^{-1}\left(\frac{E}{\Delta_1}\right)\mp\frac{\phi}{2}\right] \times\cos\left(\frac{\sqrt{E^2-\Delta_2^2}k_FL_2}{2\mu}\right)\frac{\sqrt{E^2-\Delta_2^2}}{E}=0, \tag{15}$$

where, again, the upper (lower) sign refers to the p process (n process). Taking $L_2=0$, the conditions become that of a symmetric SNS junction with a normal region of length $2L$.[8] Taking another limit, $\Delta_2=0$, the conditions become that of a symmetric SNS junction with a normal region of length $2L+L_2$. There are no tunneling features in this case due to the obvious reason that $E>\Delta_2$. The quantization conditions in the limit $E=\Delta_1$ are presented in Appendix C.

In Fig. 2, we present numerical examples of the $E(\phi)$ relations for several lengths of the middle superconductor,

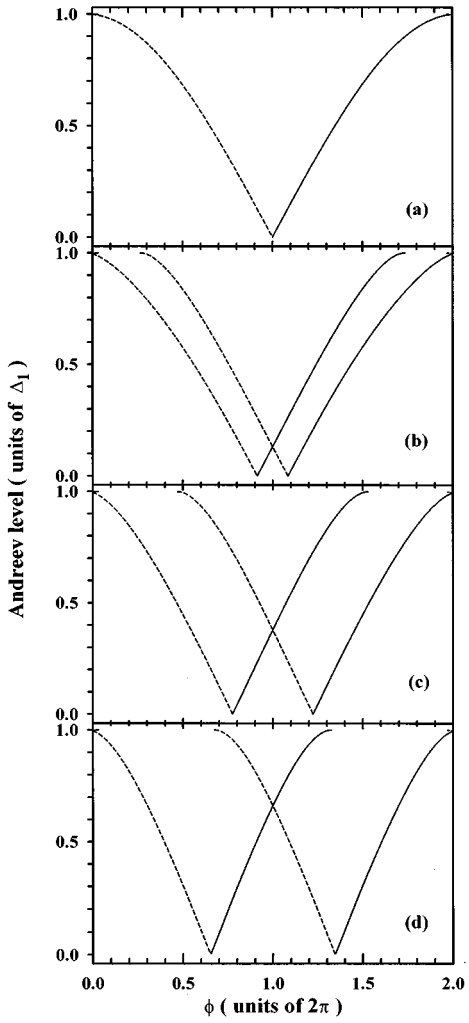

FIG. 2. Andreev levels as a function of the phase difference ϕ for a SNSNS junction with (a) $L_2=\infty$; (b) $L_2=4\xi$; (c) $L_2=2\xi$; (d) $L_2=\xi$. $\Delta_1=\Delta_2=0.2$ meV, $\mu=10$ meV, and $L=0.1\xi$. Andreev levels arise from both the p processes (————) and the n processes (– – – – –).

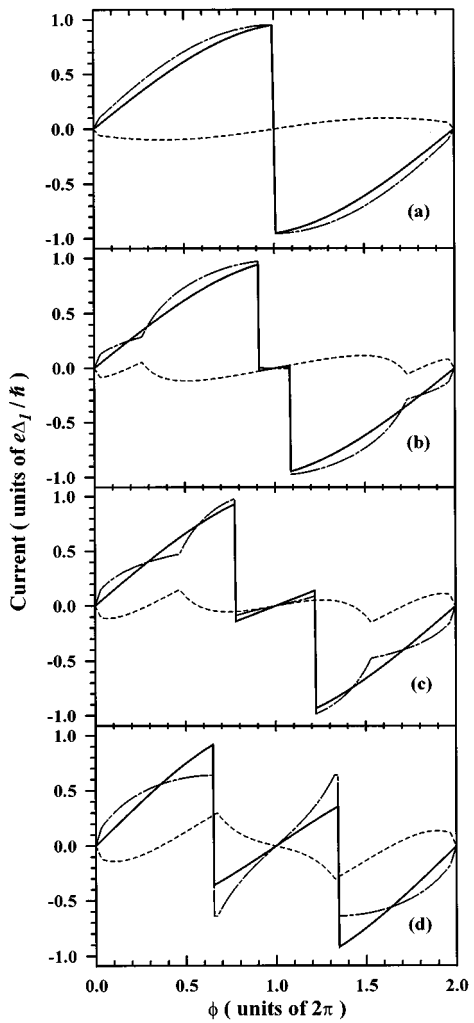

FIG. 3. Supercurrent versus phase difference ϕ across a SNSNS junction for four L_2 values and at $T=0$. The physical parameters are the same as in Fig. 2. The total current (————) consists of the current I_d due to the discrete levels (—— – ——) and the current I_s due to the scattering states (– – – – –).

with L_2 decreases from Fig. 2(a) to 2(d). The energy gaps $\Delta_1=\Delta_2=0.2$ meV, $\mu=10$ meV, temperature $T=0$, and $L=0.1\xi$, where the coherence length $\xi=\mu/k_F\Delta_1$. The ratio $\Delta_1/\mu=0.02$ is small enough for the Andreev approximation to hold. The Andreev levels from the p process are indicated by solid curves while that from the n process are indicated by dashed curves. The double degeneracy in Fig. 2(a), when L_2 is infinite, are removed when L_2 decreases, from Fig. 2(b) to 2(d). The phase separation $\Delta\phi_0$ increases when L_2 decreases. These features are consequences of the quasiparticle tunneling between the two normal regions. Near the phases ϕ when $E=0$, the $E\approx 0$ Andreev level changes from one type of process (p or n) to another type of process. This feature has important bearing on the low-temperature supercurrent characteristics.

B. Bound-state supercurrent

The supercurrent due to the Andreev levels is calculated from Eq. (9), when the summation index l includes only the bound levels. After some algebra, the bound-state current is found to be

$$I_d(\phi)=-\frac{e\hbar}{m}\sum_{\alpha=\pm 1}\sum_{E_{\alpha l}<\Delta_1}\alpha k_F\tanh(E_{\alpha l}/2k_BT)\times|a(E_{\alpha l},\alpha\phi)|^2, \tag{16}$$

where $\alpha=+1$ (-1) refers to the p process (n process), and $a(E,\phi)$ is the coefficient in Eq. (8). The $I_d(\phi)$ is shown in Fig. 3 by the dash-dotted curves for the same physical parameters used in Fig. 2. The CPR in Fig. 3(a), where L_2 is infinite, is the same as a single SNS junction except that the phase period is 4π instead of 2π. This is because of the different meaning ϕ represents. An abrupt current change occurs at $\phi=2\pi$. From Fig. 3(b) to 3(d), as L_2 decreases from 4ξ to ξ, the abrupt-current-change feature splits into two, and their phase separation increases. These current-phase characteristics are not transparent from the current expression in Eq. (16). On the other hand, there is a current expression, Eq. (11), which has been used to calculate the bound-state current in SNS junctions.[15,3,8] We evaluate Eq. (11) and show numerically that it is equal to I_d, as given by

Eq. (16). Since I_1 in Eq. (11) has the nice feature that it involves only the Andreev levels, it provides us a direct correlation between the Andreev-level-phase characteristics and the current-phase characteristics.

Before we turn our attention to the current-phase characteristics, a few more comments about I_1 is in order here. This I_1 expression was obtained by Beenakker and van Houten as one of the three terms that together give the total equilibrium current I in a superconducting point contact.[31] The other two terms are an integral over the continuous spectrum and a spatial integral. To obtain this result, they start from a relation $I=(2e/\hbar)dF/d\phi$,[32] instead of starting from Eq. (9). Here F is the free energy and ϕ is the phase difference between the two superconducting end electrodes. The derivation can be extended to the case of a superconducting junction of more general configurations by allowing the BCS interaction constant g to have spatial variation consistent with the junction configuration. The total equilibrium current I still consists of three terms—a sum over the discrete spectrum, given also by I_1, an integral over the continuous spectrum and a spatial integral. However, the spatial integral might not be small in a superconducting junction, even though it is negligible in a point contact with $L \ll \xi$,[31] where L is the length of the point contact. Thus it is not clear that the discrete sum I_1 should equal to the discrete sum I_d in Eq. (9), even though it seems probably so. Our numerical check establishes unequivocally that the two discrete sums are equal. With the establishment that $I_d=I_1$, we choose to use the I_1 expression to explain, in the following, the current-phase characteristics.

The bound-state current, in units of $e\Delta_1/\hbar$ and at zero temperature, is given by the expression $-(2/\Delta_1)\Sigma_l dE_l/d\phi$, except for the case when $E_l=0$. This expression relates the current I_d directly with the Andreev levels $E(\phi)$ through the phase derivative $-dE/d\phi$. It is clear from Fig. 2 that the contributions to I_d from the p process and the n process are opposite in sign. The phase derivative is very small when $E \lesssim \Delta_1$ and its magnitude is the largest near $E=0$. Hence the changing of one type of process to another type of process near $E \approx 0$ results in the large abrupt change in I_d. The phase separation between the abrupt-current-change feature in I_d is exactly the phase separation between the two $E=0$ Andreev levels. The same argument can be applied to understand the kinks, near, for example, $\phi \approx 0.5\pi$ and 3.5π in Fig. 3(b). The kinks are due to Andreev levels appearing near $E \approx \Delta_1$. From the above results, we have established the connection of the I_d current-phase features with the microscopic Andreev levels.

C. Scattering-state supercurrent and current-phase relations

The supercurrent due to the scattering states is calculated from Eq. (9), where the discrete sum includes only quasiparticles with $E_l > \Delta_1$. When we calculate the scattering state supercurrent I_s in the normal region N_1, the coefficients such as A_3 and A_4 in Eq. (7) are involved. However, when we calculate I_s in the normal region N_2, other coefficients such as A_7 and A_8 in Eq. (7) are involved. But, after some lengthly algebra, the I_s expressions in both of the normal regions are found to be the same, as they should. The I_s is given by

$$I_s = -\frac{2e}{h}\int_{\Delta_1}^{\sqrt{\mu^2+\Delta_1^2}} dE \frac{E}{\sqrt{E^2-\Delta_1^2}} \tanh(E/2k_BT) \times \left[\frac{\mathcal{F}_1(E,\phi/2)}{|\mathcal{D}(E,\phi/2)|^2} - \frac{\mathcal{F}_1(E,-\phi/2)}{|\mathcal{D}(E,-\phi/2)|^2}\right](u_1^2-v_1^2)^2, \tag{17}$$

where

$$\mathcal{D}(E,\theta) = \exp[i(2\tilde{k}_h L + k_{h,2}L_2 + \theta)]u_1^2u_2^2 - \exp[i(2\tilde{k}_e L + k_{e,2}L_2 - \theta)]v_1^2u_2^2 + 2\{\exp[i(\tilde{k}_h L + \tilde{k}_e L + k_{e,2}L_2)] - \exp[i(\tilde{k}_h L + \tilde{k}_e L + k_{h,2}L_2)]\}u_1u_2v_1v_2 - \exp[i(2\tilde{k}_h L + k_{e,2}L_2 + \theta)]u_1^2v_2^2 + \exp[i(2\tilde{k}_e L + k_{h,2}L_2 - \theta)]v_1^2v_2^2, \tag{18}$$

and

$$\mathcal{F}_1(E,\theta) = u_2^4 + v_2^4 - 2[-\cos(\theta + \tilde{k}_h L - \tilde{k}_e L + k_{h,2}L_2 - k_{e,2}L_2)u_1v_1u_2^3v_2 - \cos(\theta + \tilde{k}_h L - \tilde{k}_e L - k_{h,2}L_2 + k_{e,2}L_2)u_1v_1u_2v_2^3 + \cos(\theta + \tilde{k}_h L - \tilde{k}_e L)u_1v_1u_2v_2 + \cos(k_{h,2}L_2 - k_{e,2}L_2)u_2^2v_2^2]. \tag{19}$$

In Fig. 3, the dependence of the current-phase characteristics on L_2 is presented. Both the bound-state supercurrent I_d and the scattering-state supercurrent I_s have kink features, which occur at the same ϕ's and, as discussed in the previous subsection, are associated with Andreev levels appearing near $E \lesssim \Delta_1$. Remarkably, these kink features in I_d and I_s cancel each other exactly so that these features disappear from the total supercurrent. Similar exact cancellation was found also in SNS junctions,[8] but it is shown here in SNSNS junctions. Besides this nice cancellation, the other important features in the total supercurrent are the abrupt-current-change features, which are due solely to I_d. Hence, the understanding we establish in the previous subsection, about the abrupt-current-change features in I_d, can be carried over to understand the same features in the total supercurrent. The direct connection between the features in the CPR, at zero temperature, and the Andreev levels, near $E=0$, shows the importance of the CPR to the microscopic characterization of the mesoscopic superconducting junctions.

In Fig. 4, the difference in the CPR, between our results

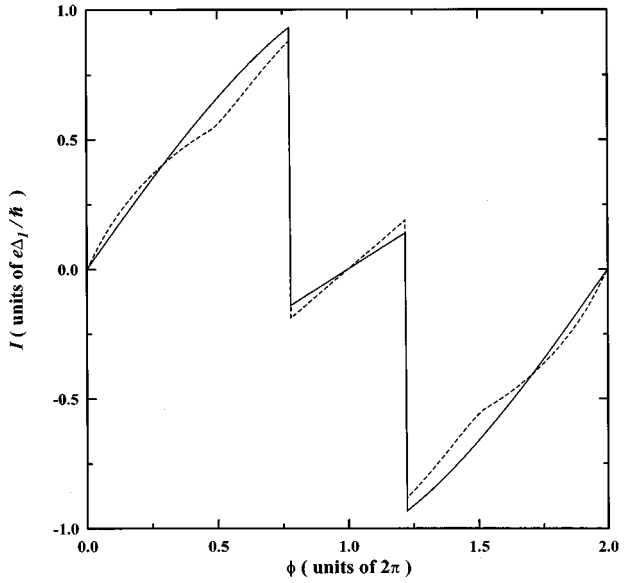

FIG. 4. Supercurrent versus phase difference ϕ. The physical parameters are the same as in Fig. 2(c). The results according to the transmission approach (– – – – –) is shown for comparison.

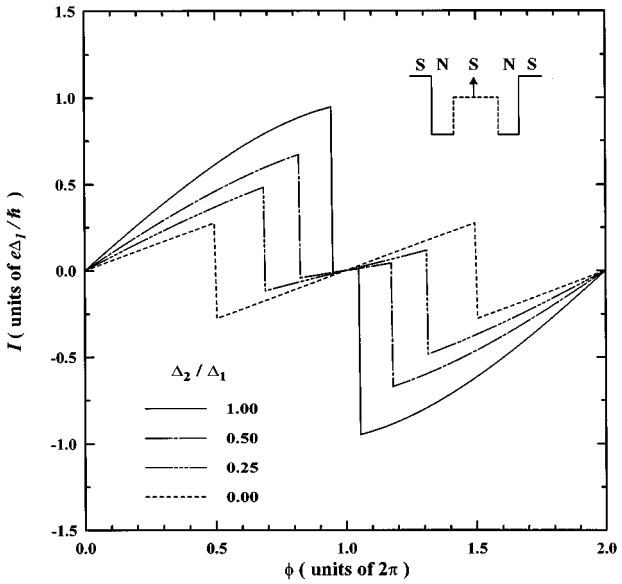

FIG. 5. Supercurrent versus phase difference ϕ for four Δ_2/Δ_1 ratios, and at $T=0$. $\Delta_1=0.2$ meV, $L_2=5\xi$, and $L=0.1\xi$.

and the results from the transmission approach, is presented. The physical parameters are the same as that in Fig. 3(c). Our results, denoted by the solid curve, are the total supercurrent I_d+I_s. The results from the transmission approach, given by the dashed curve, are I_1+I_2. The current I_2, according to Eq. (12), is found to have the same form as I_s in Eq. (17), except that $\mathcal{F}_1(E,\theta)$ is replaced by $\mathcal{F}_2(E)$, with

$$\mathcal{F}_2(E)=u_2^4+v_2^4-2\,u_2^2v_2^2. \tag{20}$$

It is straightforward to show that $\mathcal{F}_1(E,\theta)=\mathcal{F}_2(E)$ for the cases $L_2=0$ and $\Delta_2=0$. This means that our results are the same as that of the transmission approach in the SNS limit. However, in general, $\mathcal{F}_1(E,\theta)$ is not equal to $\mathcal{F}_2(E)$, and our results for the SNSNS junctions are not the same as that of the transmission approach. To demonstrate this more explicitly, we obtain the small ϕ expansion of $\Delta I=I_s-I_2$ for the special case when $\Delta_1=\Delta_2$, and when the normal regions have $L=0$. The ΔI expression, given by

$$\Delta I=-\frac{2e\phi}{h}\int_{\Delta_1}^{\sqrt{\mu^2+\Delta_1^2}}dE\,\frac{E}{\sqrt{E^2-\Delta_1^2}}\tanh(E/2k_BT)$$
$$\times\left[\frac{2\sin(k_{e,2}L_2-k_{h,2}L_2)u_1^2v_1^2}{(u_1^2-v_1^2)^2}\right], \tag{21}$$

is clearly not zero for general T and L_2. As shown in Fig. 4, in which $L=0.1\xi$, the differences are quite significant in that, besides the abrupt-current-change features, there is no kink in our results, but there are kinks in the results of the transmission approach. Moreover, the critical currents are different, and the critical current according to the transmission approach is, in this case, smaller. On the other hand, there are similar features—the abrupt-current-change features, in which the phase separation $\Delta\phi_0$ between the features is the same. It is because the bound-state current $I_d=I_1$.

The dependence of the CPR on the energy-gap configuration is presented in Fig. 5. The physical parameters are $\Delta_1=0.2$ meV, $L=0.1\xi$, $T=0$, and $L_2=5\xi$. As the ratio Δ_2/Δ_1 decreases from 1.00 to 0.0, the phase separation $\Delta\phi_0$ between the abrupt-current-change features increases. This is due to the enhancement in the Andreev-level tunneling as the pair-potential barrier of the middle superconductor lowers. There is no kink other than the abrupt-current-change features. The $\Delta_2/\Delta_1=0$ curve corresponds to a SNS junction, with the length of the normal region $2L+L_2$, and the ϕ period reduces to 2π. The critical current is the lowest in this case because the Cooper pairs have to traverse the longest effective distance through the normal region. Thus, as the Δ_2 increases, the effective length of the normal region for the Cooper pairs to traverse decreases, and the critical current increases. This trend is confirmed by the curves in Fig. 5.

We have other data for different L's, and we find that the $\Delta\phi_0$'s for the abrupt-current-change features remain the same as in Fig. 5. This shows that, within our model, the abrupt-current-change features depend only on the physical properties of the middle superconductor. That the abrupt-current-change features are independent of L can be understood in terms of the Andreev reflection. From Eq. (8), the p-process wave function in the normal region has spatial dependence involving both $\exp(i\tilde{k}_e x)$ and $\exp(i\tilde{k}_h x)$, which represent the right-going electronlike quasiparticles and the left-going holelike quasiparticles, respectively. As the quasiparticles complete a close path in the normal region, their phases change, and the change in phase involves a L-dependent term, given by $(\tilde{k}_e-\tilde{k}_h)L$. At energy $E=0$, the wave vectors $\tilde{k}_e=\tilde{k}_h=k_F$. Hence the phase change becomes L independent, and so is the $\Delta\phi_0$ for the abrupt-current-

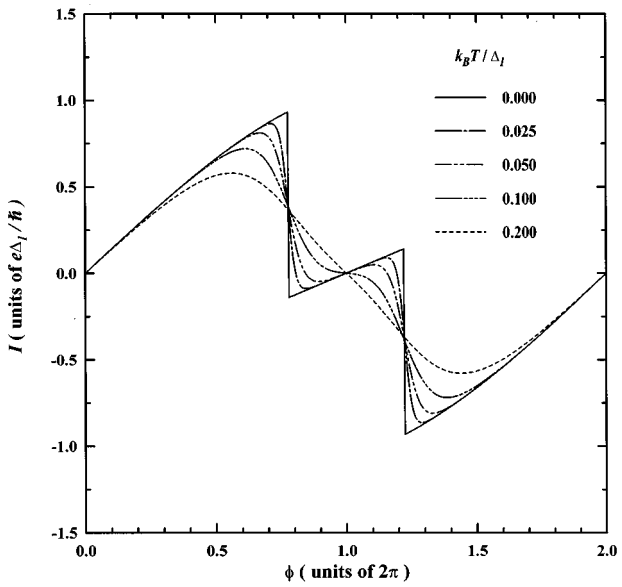

FIG. 6. Supercurrent versus phase difference ϕ for five temperatures T. $\Delta_1=\Delta_2=0.2$ meV, $L=0.1\xi$, and $L_2=2\xi$.

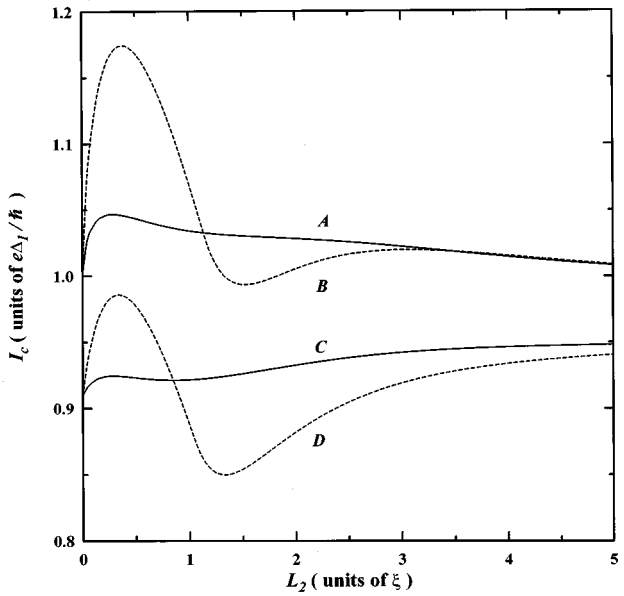

FIG. 7. Critical current versus L_2 for two SNSNS junctions and at $T=0$. $\Delta_1=\Delta_2=0.2$ meV. For the case $L=0$, our results (curve A), and the transmission results (curve B) are shown for comparison. For the case $L=0.1\xi$, our results (curve C) and the transmission results (curve D) are shown for comparison.

change features. We note that this L-independent feature cannot be obtained from normal reflection processes.

In Fig. 6, the finite-temperature effects on the CPR are presented. Within the low-temperature regime, in which the $k_BT\lesssim 0.2\Delta_1$, we can assume that the energy gaps retain their zero-temperature values. The temperature effects thus come merely from the hyperbolic tangent factors in Eqs. (16) and (17). The results show that the abrupt-current-change features remain recognizable up to $k_BT\lesssim 0.025\Delta_1$. At $k_BT\approx 0.2\Delta_1$, the features disappear, while the CPR begins to exhibit more sinusoidal-like behavior, though with a ϕ period of 4π. By then, the connection of the CPR with the microscopic Andreev levels is destroyed.

The dependence of the critical current on the length L_2 of the middle superconductor is shown in Fig. 7. The physical parameters are $\Delta_1=\Delta_2=0.2$ meV and $T=0$. Our results for $L=0$ are given by curve *A*, and the results for the transmission approach are given by curve *B*. The difference between the results from the two approaches is the largest near $L_2\approx 0.5\xi$, where the difference is more than 12%. This difference is much greater than the Andreev accuracy, given by Δ_1/μ, which is 2% in our case. The critical current from the transmission approach can be greater or smaller than our results, depending on the values of L_2. The critical current at $L_2=0$ is $e\Delta_1/\hbar$, which is the critical current of a SNS junction with zero normal region length. In the large L_2 limit, the critical current approaches $e\Delta_1/\hbar$ again, which is the result for two independent SNS junctions. We note that both curves do not exhibit oscillations on the scale of $k_FL_2\sim\pi$. This can be understood also in terms of the Andreev reflection. First of all, the critical current is essentially the current when the abrupt-current-change occurs, and is therefore closely associated with the Andreev levels at $E=0$. For a right-going electronlike quasiparticle, and at $E=0$, completing a closed path in the middle superconductor, the L_2-dependent phase change is given by $(k_{e,2}-k_{h,2})L_2$. But, from Eq. (6), when $k_{e,2}=k_F(1+i\Delta_2/2\mu)$, and $k_{h,2}=k_F(1-i\Delta_2/2\mu)$, the phase change becomes purely imaginary. This means that the effects of L_2 do not give rise to oscillations on the scale of $k_FL_2\sim\pi$. We present in curve *C* the critical current for $L=0.1\xi$ and show that the critical current is smaller, due to the effectively longer normal region distance the Cooper pairs have to traverse. The critical current at $L_2=0$ is that of a SNS junction with normal region length 0.2ξ. In the large L_2 limit, the critical current approaches that of two independent SNS junctions, each with normal region length 0.1ξ, which is 0.91 $e\Delta_1/\hbar$. The curve *C* shows that at $L_2=5\xi$, the critical current is already close to its asymptotic value. However, for the transmission results, given by curve *D*, the critical current approaches its asymptotic value in a much longer L_2.

Finally, in Fig. 8, we present the temperature dependence of the critical current. The physical parameters are $\Delta_1=\Delta_2=0.2$ meV and $L_2=0.4\xi$. The solid curves are our results and the dashed curves are the results from the transmission approach. Curves *A* and *B* are for the case $L=0$ and Curves *C*, and *D* are for the case $L=0.1\xi$. The critical current drops monotonically with the increasing of the temperature. All the four curves show a similar trend, though they differ in magnitude.

IV. CONCLUSION

We have studied the supercurrent characteristics in a symmetric SNSNS junction and have established the connection between the current-phase relation and the microscopic Andreev-level tunneling in such systems. As a consequence of Andreev reflection, the low-temperature supercurrent characteristics are shown to depend more on the physical properties of the middle superconductor and less on the normal regions as well as on the two superconducting electrodes. The importance of the current-phase relation to the

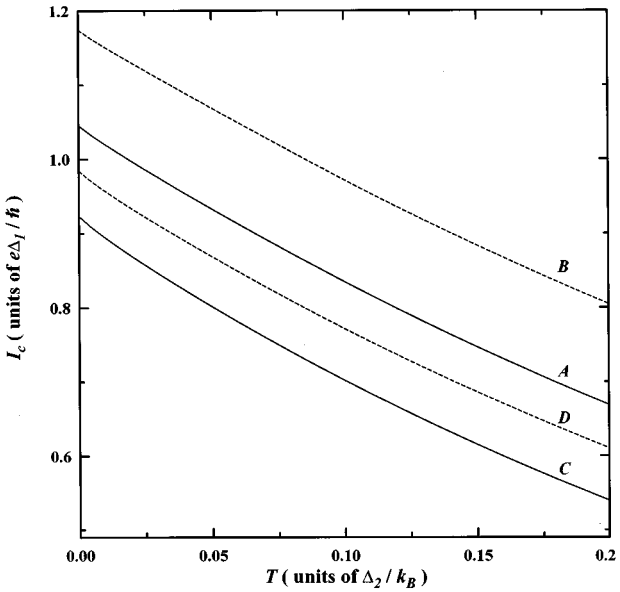

FIG. 8. Critical current versus temperature T for two SNSNS junctions. $\Delta_1=\Delta_2=0.2$ meV, $L_2=0.4\xi$. For the case $L=0$, our results (curve A) and the transmission results (curve B) are shown for comparison. For the case $L=0.1\xi$, curve C is our results and curve D is the transmission results.

microscopic characterization of the junction is pointed out and is shown to hold at the finite but low-temperature regime.

We have also demonstrated that the total current obtained from the transmission approach differs from our result in SNSNS junctions. Since the discrete sum of the two approaches are the same, the difference in the total current is from the difference between the continuous spectrum integrals in Eq. (9), and in Eq. (12), which are I_s and I_2, respectively. The difference vanishes for the case of a single SNS junction. Before we present a physical reason for the difference, we want to point out again that the current expression in I_s is microscopically derived, while that given by I_2 is not. The latter expression expresses I_2 in terms of the transmission coefficients. This amounts to evaluate, in the right superconducting electrode, the contribution to the current from the right-going quasiparticles, and, in the left superconducting electrode, the contribution from the left-going quasiparticles. In fact, imposing this view point into the evaluation of Eq. (9) does lead to I_2.[33] However, a correct evaluation of Eq. (9), as we have done so in obtaining I_s, requires us to calculate all contributions at the same location. Even though the view point that leads to I_2 is found to give the correct transport current in mesoscopic normal structures,[19] and in SNS junctions, our result for SNSNS junctions demonstrates the case when the current can no longer be expressed merely by transmission coefficients.

To understand why I_s and I_2 are different in a SNSNS junction, we first discuss how they are the same in a SNS junction. The $u^*(x)\hat{p}_x u(x)$ and the $v(x)\hat{p}_x v^*(x)$ expressions due to a left- (right-) going quasiparticle, when evaluated in the normal region of a SNS junction, are found to equal to the respective expressions, when evaluated in the left (right) superconducting electrode. These results guarantee that I_2 and I_s are equal in varying temperatures because the $u^*\hat{p}_x u$ and the $v\hat{p}_x v^*$ expressions have different temperature dependence, given by $f(E)$, and $1-f(E)$, respectively. For convenience, we choose to evaluate I_s in the normal region.

In the case of a SNSNS junction, there are two normal regions. According to the above result, the $u^*\hat{p}_x u$ and the $v\hat{p}_x v^*$ expressions due to left- (right-) going quasiparticles, when evaluated in the left (right) superconducting end-electrode, are equal to the respective expressions, when evaluated in the left (right) normal region. It is then clear that if I_s were to equal to I_2, the $u^*\hat{p}_x u$ and the $v\hat{p}_x v^*$ expressions should equal their counterparts in both of the normal regions. This, however, is not true because the middle superconductor gives rise to an additional Andreev reflection which results in converting electronlike quasiparticles into holelike quasiparticles, or vice versa, by reflection. Since the extent of the conversion depends on the energies of the quasiparticles as well as the parameters describing the junction, the $u^*\hat{p}_x u$ expression cannot maintain the same value in the two normal regions. Similarly, the $v\hat{p}_x v^*$ expressions are different in the two normal regions. Thus I_s is not equal to I_2 in a SNSNS junction.

This discrepancy in current shows that the transport current cannot be expressed merely by transmission coefficients in SNSNS junctions, in particular, and, more generally, in junctions where the additional Andreev reflection occurs within the region between the two superconducting end electrodes. On the other hand, for the case when only normal scattering, such as those caused by an impurity, occurs within the region between the two superconducting end electrodes, the same argument leads to the conclusion that I_s equals I_2. In any case, Eq. (9) gives the correct current expression.

ACKNOWLEDGMENTS

This work was supported in part by the National Science Council of the Republic of China through Contract No. NSC85-2112-M-009-015.

APPENDIX A: TRANSMISSION COEFFICIENTS

For an electronlike quasiparticle incident from the left-hand side of the junction, the $t_{e(h)}$, and the $r_{e(h)}$ coefficients in Eq. (7) are obtained, given by

$$r_e=t_h=0, \quad r_h=\frac{\mathcal{G}(E,\phi/2)}{\mathcal{D}(E,\phi/2)}, \quad t_e=\frac{\mathcal{K}_1(E,\phi/2)}{\mathcal{D}(E,\phi/2)}, \tag{A1}$$

where

$$\begin{aligned}\mathcal{G}(E,\theta)=&\exp[i(2\tilde{k}_e L+k_{e,2}L_2-\theta)]u_1v_1u_2^2-\exp[i(2\tilde{k}_h L+k_{h,2}L_2+\theta)]u_1v_1u_2^2-\exp[i(\tilde{k}_h L+\tilde{k}_e L+k_{e,2}L_2)]u_2v_2\\&+\exp[i(\tilde{k}_h L+\tilde{k}_e L+k_{h,2}L_2)]u_2v_2+\exp[i(2\tilde{k}_h L+k_{e,2}L_2+\theta)]u_1v_1v_2^2-\exp[i(2\tilde{k}_e L+k_{h,2}L_2-\theta)]u_1v_1v_2^2,\end{aligned} \tag{A2}$$

and

$$\mathcal{K}_1(E,\theta)=\exp\{i[2(\tilde{k}_h+\tilde{k}_e-k_{e,1})L+(k_{h,2}+k_{e,2})L_2 - k_{e,1}L_2-\theta]\}(u_1^2-v_1^2)(u_2^2-v_2^2). \quad \text{(A3)}$$

The transmission and the reflection coefficients are defined in terms of the $t_{e(h)}$ and the $r_{e(h)}$ coefficients, given by

$$T^e_{L\to R}(E,\theta)=|t_e|^2, \quad \text{(A4)}$$

$$R^h_{L\to R}(E,\theta)=|r_h|^2. \quad \text{(A5)}$$

We have checked that $T^e_{L\to R}+R^h_{L\to R}=1$, which is expected because the BdG equation is Hermitian.

For a holelike quasiparticle incident from the left-hand side of the junction, the $t_{e(h)}$ and the $r_{e(h)}$ coefficients are

$$r_h=t_e=0, \quad r_e=\frac{\mathcal{G}(E,-\phi/2)}{\mathcal{D}(E,-\phi/2)}, \quad t_h=\frac{\mathcal{K}_2(E,-\phi/2)}{\mathcal{D}(E,-\phi/2)}, \quad \text{(A6)}$$

where

$$\mathcal{K}_2(E,\theta)=\exp\{i[k_{h,1}(2L+L_2)+\theta]\}(u_1^2-v_1^2)(u_2^2-v_2^2). \quad \text{(A7)}$$

Again, the transmission and the reflection coefficients are defined as

$$T^h_{L\to R}(E,\theta)=|t_h|^2, \quad \text{(A8)}$$

$$R^e_{L\to R}(E,\theta)=|r_e|^2, \quad \text{(A9)}$$

where we have checked that $T^h_{L\to R}+R^e_{L\to R}=1$. From the above expressions for the $T^{e(h)}_{L\to R}$ and the $R^{e(h)}_{L\to R}$ we find the relations

$$T^h_{L\to R}(E,\theta)=T^e_{L\to R}(E,-\theta), \quad \text{(A10)}$$

and

$$R^h_{L\to R}(E,\theta)=R^e_{L\to R}(E,-\theta). \quad \text{(A11)}$$

For the cases when the quasiparticles are incident from the right-hand side of the junction, the results are the same, except that the signs of the phases are reversed. These relations are

$$T^{e(h)}_{R\to L}(E,\theta)=T^{e(h)}_{L\to R}(E,-\theta), \quad \text{(A12)}$$

and

$$R^{e(h)}_{R\to L}(E,\theta)=R^{e(h)}_{L\to R}(E,-\theta). \quad \text{(A13)}$$

We note that our results are for general normal-region length L. Our transmission coefficients reduce to that obtained by Hurd and Wendin[18] when taking the $L=0$ limit.

APPENDIX B: MICROSCOPIC DERIVATION OF EQ. (9)

The electron field operators $\hat{\Psi}(\vec{r},\sigma)$ are related to the quasiparticle operators $\hat{\gamma}_{l,\sigma}$, and $\hat{\gamma}^\dagger_{l,\sigma}$[30]

$$\hat{\Psi}(\vec{r},\sigma)=\sum_l [\hat{\gamma}_{l,\sigma}u_l(\vec{r})-\sigma\hat{\gamma}^\dagger_{l,-\sigma}v_l^*(\vec{r})], \quad \text{(B1)}$$

where l refers to the quasiparticle states in Eq. (2), and σ is the spin index, with $\sigma=+1$ (-1) corresponding to spin up (down) electrons. The electric current density operator $\vec{j}_{\rm op}(\vec{r},\sigma)$ in the second quantized form is given by

$$\vec{j}_{\rm op}(\vec{r},\sigma)=\frac{e}{2m}\int d\vec{r}_e\hat{\Psi}^\dagger(\vec{r}_e,\sigma)\left[\left(\vec{p}-\frac{e}{c}\vec{A}\right)\delta(\vec{r}-\vec{r}_e)+\delta(\vec{r}-\vec{r}_e)\left(\vec{p}-\frac{e}{c}\vec{A}\right)\right]\hat{\Psi}(\vec{r}_e,\sigma). \quad \text{(B2)}$$

Here, the $\vec{p}$ and $\vec{A}$ are both functions of $\vec{r}_e$. After performing the integration, the current density operator

$$\vec{j}_{\rm op}(\vec{r},\sigma)=\frac{e}{2m}\left[\hat{\Psi}^\dagger(\vec{r},\sigma)\left(\vec{p}-\frac{e}{c}\vec{A}\right)\hat{\Psi}(\vec{r},\sigma)-\left\{\left(\vec{p}+\frac{e}{c}\vec{A}\right)\hat{\Psi}^\dagger(\vec{r},\sigma)\right\}\hat{\Psi}(\vec{r},\sigma)\right], \quad \text{(B3)}$$

where $\vec{p}$ and $\vec{A}$ become functions of $\vec{r}$. The electron field operators in Eq. (B3) can be expressed in terms of the quasiparticle operators, using Eq. (B1), and are given by

$$\vec{j}_{\rm op}(\vec{r},\sigma)=\frac{e}{2m}\sum_{l,l'}[\hat{\gamma}^\dagger_{l,\sigma}u_l^*(\vec{r})-\sigma\hat{\gamma}_{l,-\sigma}v_l(\vec{r})]\left(\vec{p}-\frac{e}{c}\vec{A}\right)[\hat{\gamma}_{l',\sigma}u_{l'}(\vec{r})-\sigma\hat{\gamma}^\dagger_{l',-\sigma}v_{l'}^*(\vec{r})] - \frac{e}{2m}\sum_{l,l'}\left\{\left(\vec{p}+\frac{e}{c}\vec{A}\right)[\hat{\gamma}^\dagger_{l,\sigma}u_l^*(\vec{r})-\sigma\hat{\gamma}_{l,-\sigma}v_l(\vec{r})]\right\}[\hat{\gamma}_{l',\sigma}u_{l'}(\vec{r})-\sigma\hat{\gamma}^\dagger_{l',-\sigma}v_{l'}^*(\vec{r})]. \quad \text{(B4)}$$

The summation involves quasiparticles with energies $E_l, E_{l'} > 0$. The thermal averaged current density $\vec{j}(\vec{r}) = \Sigma_\sigma \langle \vec{j}_{\rm op}(\vec{r},\sigma)\rangle$, which can be evaluated using the thermal average properties of the quasiparticle operators[30]

$$\langle \hat{\gamma}^\dagger_{l,\sigma} \hat{\gamma}_{l',\sigma}\rangle = f(E_l)\,\delta_{l,l'},$$

$$\langle \hat{\gamma}_{l,\sigma} \hat{\gamma}^\dagger_{l',\sigma}\rangle = [1-f(E_l)]\,\delta_{l,l'}. \tag{B5}$$

The thermal averaged current density $\vec{j}(\vec{r})$ is then given by

$$\vec{j}(\vec{r}) = \frac{e}{m}\sum_l \left\{ f(E_l) u_l^*(\vec{r}) \left(\vec{p} - \frac{e}{c}\vec{A}\right) u_l(\vec{r}) + [1-f(E_l)] v_l(\vec{r}) \times \left(\vec{p} - \frac{e}{c}\vec{A}\right) v_l^*(\vec{r})\right\} + \text{c.c.} \tag{B6}$$

Equation (B6) becomes Eq. (9) in the text when the system is one dimensional and the vector potential $\vec{A} = 0$. A more general form for the equilibrium average of a single-electron operator can be found in Ref. 31.

APPENDIX C: QUANTIZATION CONDITION ($E = \Delta_1$)

Both the bound-state supercurrent I_d and the scattering-state supercurrent I_s have kink features which occur at the ϕ's when Andreev levels appear at $E = \Delta_1$. The conditions for finding these ϕ's are given by

$$\frac{\phi}{2} + 2\pi n = \pm\left(\frac{\Delta_1}{\mu} k_F L + \tan^{-1}\beta - \sin^{-1}\gamma\right),$$

$$\frac{\phi}{2} + 2\pi n = \pm\left(\frac{\Delta_1}{\mu} k_F L + \tan^{-1}\beta + \sin^{-1}\gamma - \pi\right), \tag{C1}$$

where n is an integer, and the upper (lower) sign represents the condition for the p process (n process). Here,

$$\beta = \tan\left(\frac{\sqrt{\Delta_1^2 - \Delta_2^2}\, k_F L_2}{2\,\mu}\right) \Big/ \sqrt{1 - \left(\frac{\Delta_2}{\Delta_1}\right)^2}, \tag{C2}$$

and

$$\gamma = \frac{(\Delta_2/\Delta_1)\sin[(\sqrt{\Delta_1^2 - \Delta_2^2}\, k_F L_2)/2\,\mu]}{\sqrt{1 - \{(\Delta_2/\Delta_1)\cos[(\sqrt{\Delta_1^2 - \Delta_2^2}\, k_F L_2)/2\mu]\}^2}}. \tag{C3}$$

[1] See the review by T.M. Klapwijk, Physica B **197**, 481 (1994), and the conference papers in **203**, 201 (1994).
[2] B.L. Al'tshuler and B.Z. Spivak, Zh. Éksp. Teor. Fiz. **92**, 609 (1987) [Sov. Phys. JETP **65**, 343 (1987)].
[3] C.W.J. Beenakker, Phys. Rev. Lett. **67**, 3836 (1991).
[4] C.W.J. Beenakker and H. van Houten, Phys. Rev. Lett. **66**, 3056 (1991).
[5] A. Furusaki, H. Takayanagi, and M. Tsukada, Phys. Rev. Lett. **67**, 132 (1991).
[6] H. Takayanagi, J.B. Hansen, and J. Nitta, Phys. Rev. Lett. **74**, 166 (1995).
[7] H. Takayanagi, T. Akazaki, and J. Nitta, Phys. Rev. Lett. **75**, 3533 (1995).
[8] P.F. Bagwell, Phys. Rev. B **46**, 12 573 (1992).
[9] A. Martín-Rodero, F.J. García-Vidal, and A.L. Yeyati, Phys. Rev. Lett. **72**, 554 (1994).
[10] U. Gunsenheimer, U. Schüssler, and R. Kümmel, Phys. Rev. B **49**, 6111 (1994).
[11] M. Hurd and G. Wendin, Phys. Rev. B **49**, 15 258 (1994).
[12] L.F. Chang and P.F. Bagwell, Phys. Rev. B **49**, 15 853 (1994).
[13] F. Sols and J. Ferrer, Phys. Rev. B **49**, 15 913 (1994).
[14] A.L. Yeyati, A. Martín-Rodero, and F.J. García-Vidal, Phys. Rev. B **51**, 3743 (1995).
[15] A.F. Andreev, Zh. Éksp. Teor. Fiz. **46**, 1823 (1964) [Sov. Phys. JETP **19**, 1228 (1964)].
[16] L.Y. Gorelik, V.S. Shumeiko, R.I. Shekhter, G. Wendin, and M. Jonson, Phys. Rev. Lett. **75**, 1162 (1995).
[17] F. Sols, J. Ferrer, and I. Zapata, Physica B **203** 467 (1994); I. Zapata and F. Sols, Phys. Rev. B **53**, 6693 (1996).
[18] M. Hurd and G. Wendin, Phys. Rev. B **51**, 3754 (1995).
[19] C.W.J. Beenakker and H. van Houten, in *Solid State Physics: Advances in Research and Applications*, edited by H. Ehrenreich and D. Turnbull (Academic, New York, 1991), Vol. 44, p. 1.
[20] C.J. Lambert, J. Phys. Condens. Matter **3**, 6579 (1991).
[21] B.J. van Wees, K.-M.H. Lenssen, and C.J.P.M. Harmans, Phys. Rev. B **44**, 470 (1991).
[22] Y. Takane and H. Ebisawa, J. Phys. Soc. Jpn. **61**, 1685 (1992).
[23] A.F. Morpurgo and F. Beltram, Phys. Rev. B **50**, 1325 (1994).
[24] S.J. Robinson, C.J. Lambert, and M. Jeffery, Phys. Rev. B **50**, 9611 (1994).
[25] N.R. Claughton, R. Raimondi, and C.J. Lambert, Phys. Rev. B **53**, 9310 (1996).
[26] E.de Wolff, H.C. Roobeek, M.C. Koops, and R. de B. Ouboter, Physica B **179**, 295 (1992).
[27] M.C. Koops, L. Feenstra, B.J. Vleeming, A.N. Omelyanchouk, R. de B. Ouboter, Physica B **218**, 145 (1996).
[28] S. Kashiwaya, Y. Tanaka, M. Koyanagi, and K. Kajimura, Jpn. J. Appl. Phys. **34**, 4555 (1995).
[29] J. Bardeen, R. Kümmel, A.E. Jacobs, and L. Tewordt, Phys. Rev. **187**, 556 (1969).
[30] P.G. de Gennes, *Superconductivity of Metals and Alloys* (Benjamin, New York, 1966), pp. 140–142.
[31] C.W.J. Beenakker and H. van Houten, in *Nanostructures and Mesoscopic Systems*, edited by W.P. Kirk and M.A. Reed (Academic, New York, 1992), p. 481.
[32] P.W. Anderson, in *The Many-Body Problem*, edited by E.R. Caianiello (Academic, New York, 1964), Vol. 2, p. 113.
[33] C.S. Chu and V.C.Y. Chang (unpublished).